Effects of grout and energy-dissipating bar properties on a Type III grouted seismic connection for precast concrete structures

Theresa C. Aragon, Yahya C. Kurama, and Donald F. Meinheit

- ■ This paper discusses the testing of six specimens with grouted energy-dissipating reinforcing bars forming the connection across the gap-opening joint in the precast concrete structure. The effects of grout and energy-dissipating bar properties on the connection performance are investigated.

- ■ The connection test results show that additional requirements should be introduced in ASTM A706 to improve the low-cycle fatigue performance of reinforcing bars intended for seismic applications.

- ■ There is no simple correlation between the connector grout properties and the bond pull-out performance of the connection under cyclic loading. Thus, it may be necessary to increase the bond length of the energy-dissipating bar for this nonproprietary connection to be used without the requirement for a specific grout product.

Precast concrete building and bridge structures with gap-opening joints (commonly known as rocking joints) that allow large lateral displacements have been successfully developed for seismic regions.[1–3] An important component for lateral strength and energy dissipation in these systems is the ductile deformed reinforcing bars crossing the gap-opening joints between the base of the structure and the foundation (for example, column, shear wall, and bridge pier bases). These bars are designed to undergo repetitive tension-compression yielding to provide energy dissipation during a large earthquake. A predetermined length of each energy-dissipating bar is unbonded from the concrete (by wrapping the bar inside a plastic sleeve) above or below the gap-opening joint to minimize the concentration of inelastic strains in the bar. The length of this unbonded region (also referred to as the stretch length) is selected so that the maximum steel strain in tension is within the intended range of $0.5\varepsilon_{uel}$ (to provide adequate energy dissipation) and $0.85\varepsilon_{uel}$ (to prevent low-cycle fatigue fracture),[2,4] where ε_{uel} is the uniform elongation strain of the bar (that is, the strain at the maximum strength f_{uel}) under monotonic loading.

Using this concept, a precast concrete wall system was recently validated[4,5] based on ACI's *Building Code Requirements for Structural Concrete (ACI 318-14) and Commentary (ACI 318R-14)*[6] as a special shear wall following the requirements in *Acceptance Criteria for Special Unbonded Post-Tensioned Precast Structural Walls Based on Validation Testing and Commentary* (ACI ITG-5.1).[7] One of the wall

test specimens with Type II grouted mechanical splices for the energy-dissipating bar connections to the foundation failed prematurely due to bond pullout of the energy-dissipating bars from the splice sleeve. Thus, to reach the required energy-dissipating bar strains without pullout under cyclic loading, the bars needed to be grouted over the full ACI 318-14[6] development length inside the foundation. This fully grouted detail resulted in a large amount of field grouting and long energy-dissipating bar lengths protruding out of the precast concrete wall panel base, making production, transportation, and erection more cumbersome.

Responding to the need for a higher-performing (called *Type III* here) connection for anchoring energy-dissipating bars with short grouted embedment lengths in gap-opening precast concrete joints, Aragon et al.[8] presented the results from six specimens investigating a new tapered cylindrical grouted seismic connection. The goal of this Type III connection is to allow cyclically loaded energy-dissipating bars to reach close to their full ultimate tensile strength and corresponding strain. Toward this goal, Aragon et al.[8] showed that the tested bond length of 10 times the nominal bar diameter d_b was adequate to reach large cyclic energy-dissipating bar strains. However, this finding was limited to only one grout product, one energy-dissipating bar size (no. 7 [22M]), and one steel manufacturing heat for the initial six experiments (specimens 1 through 6). Importantly, two of the specimens, 2 and 6, experienced low-cycle fatigue fracture prior to reaching the maximum allowable strain of $0.85\varepsilon_{uel}$ suggested by *Requirements for Design of a Special Unbonded Post-tensioned Precast Shear Wall Satisfying ACI ITG-5.1 and Commentary* (ACI ITG-5.2).[2] This paper extends the previous experimental program to additional test parameters involving different grout products, grout strengths, energy-dissipating bar sizes, and energy-dissipating bar heats.

Overview of experimental program

The same test setup from Aragon et al.[8] was used for the six additional specimens (specimens 7 through 12) described in this paper. Each connection specimen (**Fig. 1**) consisted of a wall-panel block and a foundation block that were cast separately and then connected using a single energy-dissipating bar with a grouted connector sleeve at the top and centered in the foundation block. During testing, the foundation block was fixed to the laboratory strong floor, and the wall-panel block was moved vertically to subject the energy-dissipating bar to a rigorous quasi-static cyclic axial strain history (Fig. 1). The strain history varied slightly between tests but in general was consistent with the recommended loading for the validation of energy-dissipating bar connections in gap-opening joints of precast concrete walls for seismic applications.[4,8]

The connector sleeve and energy-dissipating bar properties for specimens 7 through 12 are summarized in **Table 1**. Similar information for the previous specimens 1 through 6 can be found in Aragon et al.[8] A no. 7 (22M) Grade 60 (414 MPa) *Standard Specification for Deformed and Plain Low-Alloy Steel Bars for*

Concrete Reinforcement (ASTM A706)[9] reinforcing bar (d_b = 0.875 in. [22.22 mm]) served as the energy-dissipating bar to connect the wall-panel and foundation blocks for specimens 7 through 10. A no. 9 (29M) (d_b = 1.128 in. [28.65 mm]) and a no. 11 (36M) (d_b = 1.410 in. [35.81 mm]) Grade 60 ASTM A706 reinforcing bar served as the energy-dissipating bar for specimens 11 and 12, respectively.

The wall-panel block (**Fig. 2**) had a thickness t_w of 15 in. (380 mm) and length l_w of 24 in. (610 mm), representing a portion of a precast concrete wall panel at its base connection to the foundation. Each wall-panel block was reinforced with nominal no. 3 (10M) deformed Grade 60 (414 MPa) *Standard Specification for Deformed and Plain Carbon-Steel Bars for Concrete Reinforcement* (ASTM A615)[10] bars similar to the reinforcement described by Aragon et al.[8] for specimens 1 through 6. The height of the block h_w was governed by the hooked energy-dissipating bar development length, based on section 25.4.3 of ACI 318-14.[6] The height of the block h_w was 32 in. (810 mm) for specimens 7 through 10 with no. 7 (22M) energy-dissipating bars and 48 in. (1220 mm) for specimens 11 and 12 with no. 9 and 11 (29M and 36M) bars. The 90-degree hook (Fig. 2) was needed for full development at the top of the energy-dissipating bar inside the wall-panel block but would not be necessary in a full-scale/full-height precast concrete wall panel in practice. The large height of a full-sized panel would allow full development using a straight bar. The no. 7 energy-dissipating bars used 90-degree hooks, while the no. 9 and 11 bars had 180-degree hooks.

Each energy-dissipating bar was unbonded from the concrete over a length of $12d_b$ (Table 1) at the bottom of the wall-panel block by wrapping it inside a plastic sleeve. This wrapped length l_{sw} was where the yielding of the bar was designed to develop and was chosen to achieve the following:

- result in significant yielding and elongation of the bar before failure, thus allowing measurable separation at the horizontal joint between the wall-panel block and the foundation block

- reduce the effect of any additional bar debonding (due to the cyclic loading of the bar) on the steel strains determined from the measured joint separation and the wrapped length

The wrapped length of each bar was supported laterally by the surrounding wall-panel concrete, preventing buckling upon reversal of load into compression. As the bar was pulled in tension, gap opening between the wall-panel and foundation blocks exposed some of this unbonded length. However, the exposed length was not long enough to cause buckling. The restraining columns and angles of the test setup[8] prevented rotation of the wall-panel block during compression loading, thus ensuring uniaxial loading of the energy-dissipating bar.

Figure 2 shows the foundation block with a width w_f of 24 in. (610 mm), height h_f of 36 in. (910 mm), and length l_f of
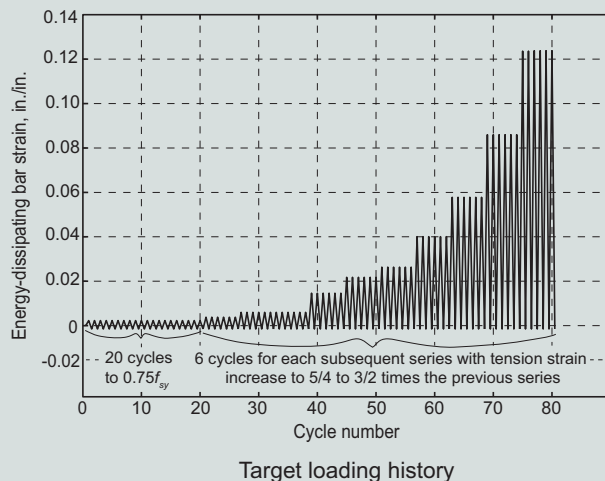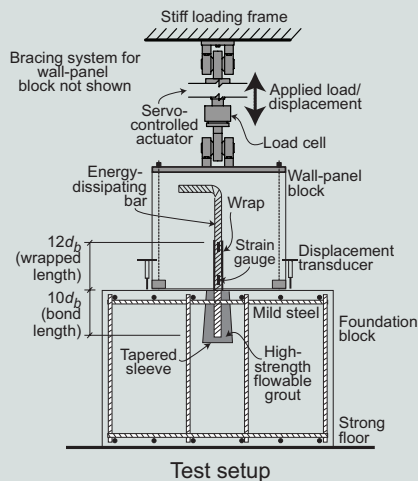
Figure 1. Energy-dissipating bar connection tests. Note: d_b = nominal diameter of energy-dissipating bar; f_{sy} = yield strength of energy-dissipating bar under monotonic tension loading. 1 in. = 25.4 mm.

Table 1. Connector sleeve, energy-dissipating bar, and connection grout properties (specimens 7 through 12)

		Specimen					
		7	8	9	10	11	12
Connector sleeve	Taper angle θ_d, degrees	4.5	4.5	0.0	4.5	4.5	4.5
	Entrance (top) diameter, in.	2.75	2.75	2.75	2.75	3.00	3.25
	Bottom diameter, in.	4.50	4.50	2.75	4.50	5.125	5.75
	Surface corrugations	None	None	Automated corrugations	None	None	None
	Length, in.	11.0	11.0	11.0	11.0	13.5	16.0
Energy-dissipating bar	Size	No. 7	No. 7	No. 7	No. 7	No. 9	No. 11
	Wrapped length l_{sw}, in.	10.5 ($12d_b$)	10.5 ($12d_b$)	10.5 ($12d_b$)	10.5 ($12d_b$)	13.5 ($12d_b$)	16.9 ($12d_b$)
	Bond length l_b, in.	8.75 ($10d_b$)	8.75 ($10d_b$)	8.75 ($10d_b$)	8.75 ($10d_b$)	11.28 ($10d_b$)	14.10 ($10d_b$)
Connection grout	Grout product	GM2	GM3	GM2	GM2	GM2	GM2
	Target 28-day compressive strength, psi	8000	8000	8000	< 8000	8000	8000
	Flow diameter, in.	5.25	5.75	5.375	9.75	5.75	6.00
	Average 28-day compressive strength f'_{cg28d}, psi	8835	8224	7821	7320	7783	8107
	Average test-day compressive strength f'_{cg}, psi	8890	8345	8427	7721	8595	8310
	Test-day age	39	59	41	40	73	78

Note: d_b = nominal diameter of reinforcing bar. No. 7 = 22M; no. 9 = 29M; no. 11 = 36M; 1 in. = 25.4 mm; 1 psi = 6.895 kPa.
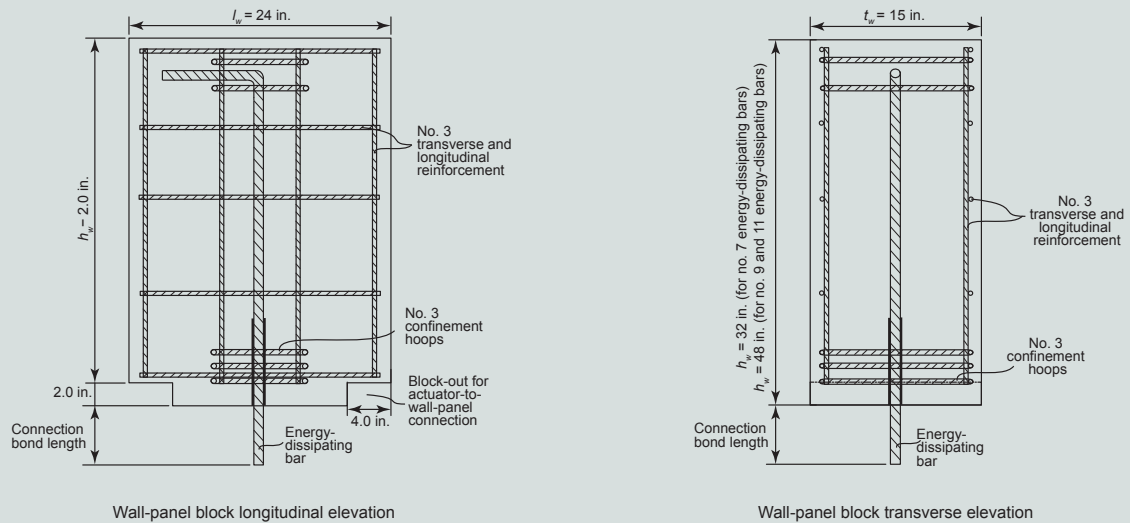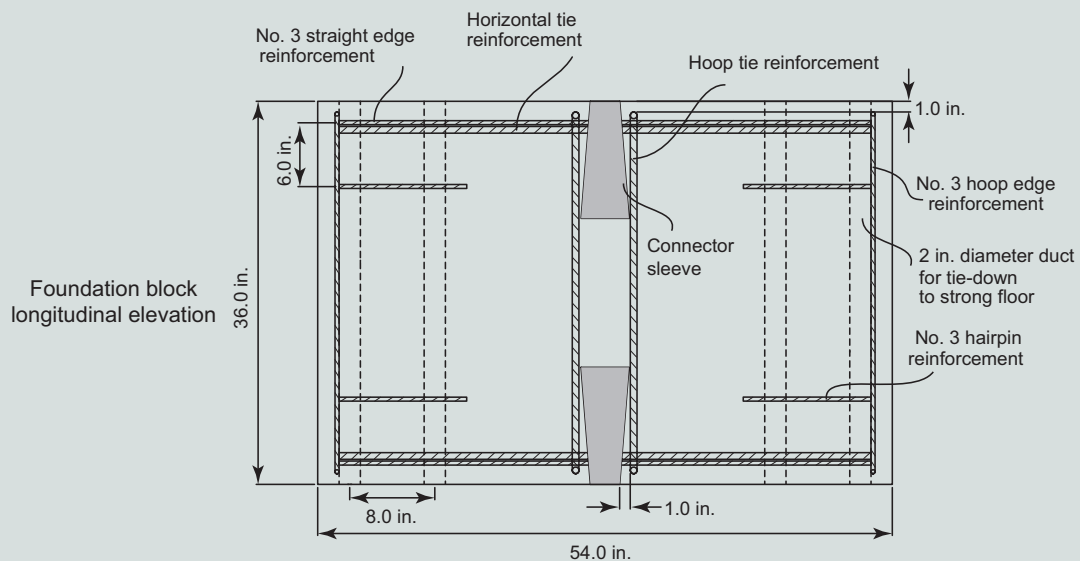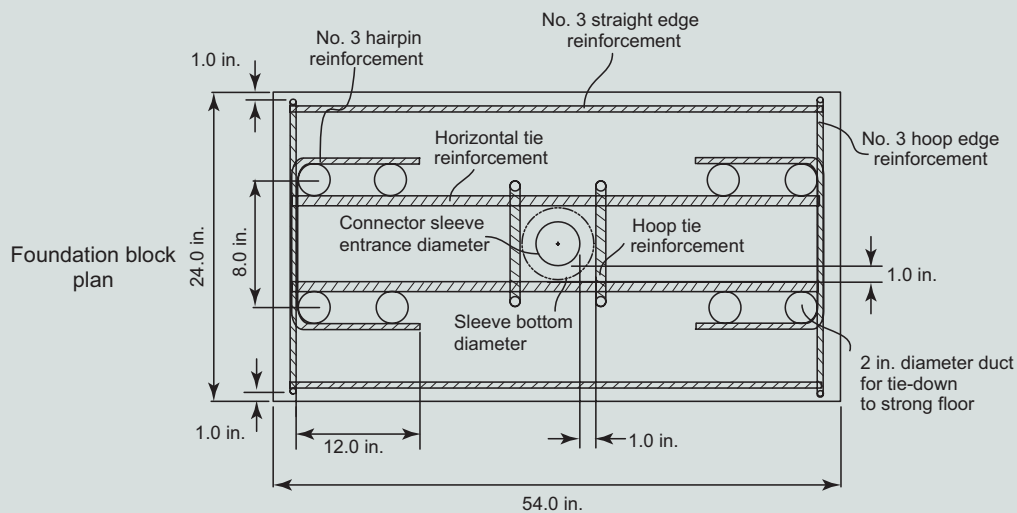
Figure 2. Wall-panel block and foundation block dimensions and reinforcement. Note: See Table 1 for energy-dissipating bar and connector sleeve information. See Table 2 for tie reinforcement information. h_f = height of foundation block; h_w = height of wall-panel block; l_f = length of foundation block; l_w = length of wall-panel block; t_w = thickness of wall-panel block; w_f = width of foundation block. No. 3 = 10M; no. 7 = 22M; no. 9 = 29M; no. 11 = 36M; 1 in. = 25.4 mm.

54 in. (1370 mm). Each foundation block was designed to be reused in two tests and accommodate two energy-dissipating bar connector sleeves (one on the top and one on the bottom of the block) by rotating the top of the block with respect to the bottom after the completion of a test. Deformed ASTM A615 Grade 60 (414 MPa) vertical (hoop) tie and horizontal tie reinforcement was placed around each connector sleeve to prevent breakout of the concrete surrounding the energy-dissipating bar connection. **Table 2** shows the tie reinforcement for the different energy-dissipating bar sizes. Details on the strut-and-tie model used in the design of this tie reinforcement can be found in Aragon et al.[8]

Energy-dissipating bar connection properties

The connector sleeves used in specimens 7 through 12 are shown in **Fig. 3** and listed in Table 1. Except for specimen 9, the sleeves were made by a local sheet metal manufacturer using light-gauge smooth sheet metal with a thickness of 0.0209 in. (0.531 mm) (gauge 25). Each sleeve used a spot-welded lap joint that was not intended to provide confinement. Note that although the metal sleeve itself did not provide confinement to the grout, the surrounding foundation concrete did provide confinement due to the tapered shape of the connection. As the reinforcing bar was pulled, the surrounding concrete restrained the tapered grout cone from pulling out of the sleeve. This restraint resulted in confining stresses at the top (narrow) end of the grout cone.

The straight sleeve in specimen 9 was a commercially available corrugated steel pipe typically used in the post-tensioning industry. The sleeve corrugations in specimen 9 were much larger than those in the corrugated sleeves in specimens 2 through 6,[8] which were placed manually during the manufacturing of the sleeves from smooth sheet metal. For practical tolerance purposes, the sleeves were fabricated to be slightly longer than the embedment bond length ($10d_b$) of the energy-dissipating bars. Further, the diameter of the top end for each sleeve (energy-dissipating bar entry end) was oversized to provide adequate clearance and tolerance for the placement of the energy-dissipating bars in the field.

As described in detail in Aragon et al.,[8] for each specimen, a 55 lb (25 kg) bag of prepackaged grout was mixed using a drill mixer per manufacturer instructions to reach a flowable consistency. All of the grout products were hydraulic, cement-based, nonshrink grouts that met the requirements of *Standard Specification for Packaged Dry, Hydraulic-Cement Grout (Nonshrink)* (ASTM C1107)[11] (Grades A, B, and C) and were specified for a wide range of applications, including the grouting of anchor bolts, reinforcing bars, and dowel rods. Prior to placement inside the connector sleeve, the consistency of the grout was checked to ensure that there was no separation or other undesirable behavior. The flow diameter (spread) of each batch was measured using a 2 in. (50 mm) diameter by 4 in. (100 mm) tall plastic tube that was filled with grout and slowly lifted on top of a flow template. Upon confirmation that the grout satisfied the target spread diameter (described later), it was gravity fed manually into the connector sleeve and a tamping rod was used to ensure that the grout was properly placed with no voids.

One of the experimental variables in this series of tests was the connection grout placed inside the sleeves, as shown in Table 1. To examine the effect of different grout products and manufacturers, specimens 7 and 8 used the same energy-dissipating bar size (no. 7 [22M]), bond length ($10d_b$), and connector sleeve dimensions (top diameter of 2.75 in. [70 mm] and length of 11 in. [280 mm]) as in specimen 1,[8] except that different grout products were used (GM2 and GM3 in specimens 7 and 8, respectively, compared with GM1 used in specimen 1). Results from a microscopic characterization of these three grout products are discussed later in this paper. The target grout spread diameter for specimens 7 and 8 was 5 to 6 in. (125 to 150 mm), as in specimen 1. The average connection test-day grout compressive strengths f'_{cg} in specimens 7 and 8 were 8890 psi (61.3 MPa) and 8345 psi (57.54 MPa), respectively, and were smaller than the grout strength f'_{cg} of 9498 psi (65.49 MPa) in specimen 1.

The straight connector sleeve in specimen 9 had similar overall dimensions to the straight sleeve in specimen 5 from Aragon et al.[8] The grout in specimen 5 had a very high test-day average compressive strength f'_{cg} of 10,324 psi (71.18 MPa), and therefore a lower grout average compressive strength was investigated in specimen 9 (f'_{cg} = 8427 psi [58.10 MPa]) using GM2. In addition, the corrugations on the connector sleeve in specimen 9 were much deeper and more closely spaced than the corrugations in specimen 5.

Table 2. Foundation block tie reinforcement

Energy-dissipating bar size	Horizontal tie reinforcement		Hoop tie reinforcement	
	Reinforcement	Total area, in.²	Reinforcement	Total area, in.²
No. 7	Two no. 5 bars	0.62	Two no. 5 hoops	1.24
No. 9	Two no. 6 bars	0.88	Two no. 6 hoops	1.76
No. 11	Two no. 5 plus two no. 6 bars	1.50	Four no. 5 hoops	2.48

Note: No. 5 = 16M; no. 6 = 19M; no. 7 = 22M; no. 9 = 29M; no. 11 = 36M; 1 in.² = 645.2 mm².
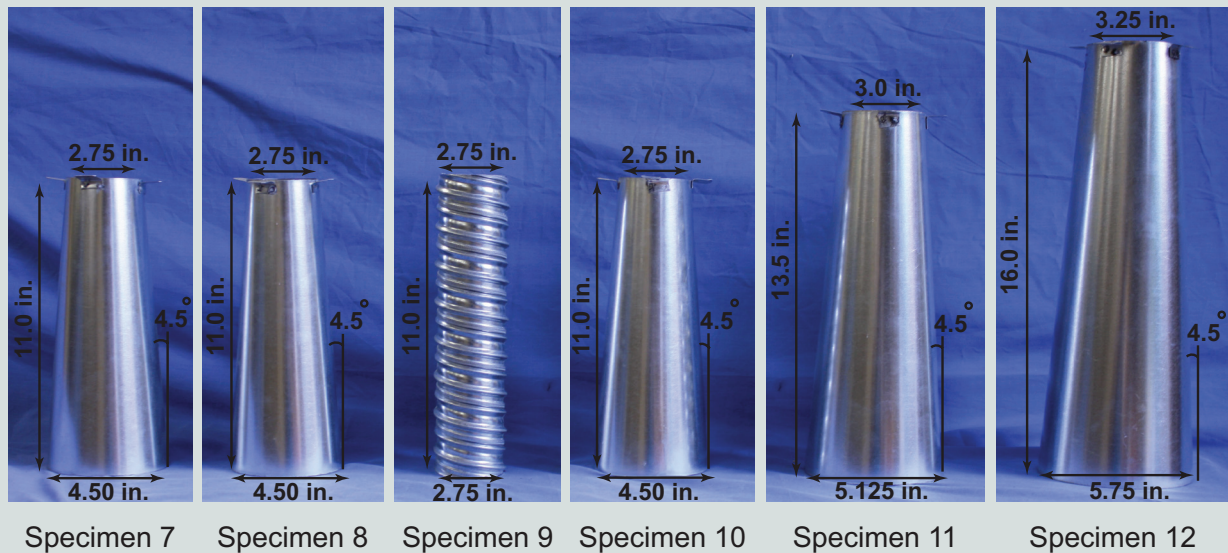
Figure 3. Connector sleeve dimensions (specimens 7 through 12). Note: 1 in. = 25.4 mm.

Specimen 10 used the same connector sleeve geometry as in specimens 7 and 8, but with a target grout compressive strength lower than 8000 psi (55.2 MPa). An increased amount of water was added during the mixing of the grout (simulating a possible field construction error) to achieve the lower strength, resulting in a grout spread diameter of 9.75 in. (250 mm) and a grout average compressive strength f'_{cg} of 7721 psi (53.24 MPa) using GM2.

The connectors in specimens 11 and 12 used no. 9 and 11 (29M and 36M) energy-dissipating bars, respectively. The connector sleeve taper angle remained the same as the other tapered sleeves (θ_d = 4.5 degrees), but the top (energy-dissipating bar entry) diameter (3.0 in. [75 mm] and 3.25 in. [83 mm]) and length (13.5 in. [340 mm] and 16.0 in. [410 mm]) of the sleeve were increased to accommodate the larger no. 9 and 11 energy-dissipating bar diameters, respectively. The bond length of the energy-dissipating bar was kept at $10d_b$ (11.3 in. [287 mm] and 14.1 in. [358 mm] for the no. 9 and 11 bars, respectively). The average connection test-day grout compressive strengths f'_{cg} using GM2 were 8595 and 8310 psi (59.26 and 57.3 MPa) in specimens 11 and 12, respectively.

Energy-dissipating bar stress-strain properties

The monotonic tension stress-strain behavior of the Grade 60 (414 MPa) ASTM A706 energy-dissipating reinforcement was determined by testing sample bars in a hydraulic universal testing machine. The bar strains in these monotonic material tests were measured using an extensometer with a 2 in. (50 mm) gauge length placed over the free length of each bar (in between the end grips of the testing machine). The extensometer was removed prior to bar fracture (to prevent damage to the extensometer) but after the bar had reached the maximum
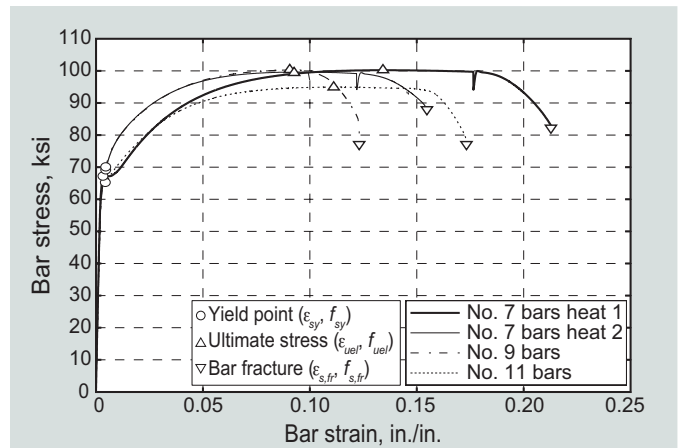
Figure 4. Energy-dissipating bar stress-strain behaviors under monotonic tension. Note: $f_{s,fr}$ = stress of energy-dissipating bar at fracture under monotonic tension loading; f_{sy} = yield strength of energy-dissipating bar under monotonic tension loading; f_{uel} = ultimate (maximum) strength of energy-dissipating bar under monotonic tension loading; $\varepsilon_{s,fr}$ = strain of energy-dissipating bar at fracture under monotonic tension loading; ε_{sy} = yield strain of energy-dissipating bar under monotonic tension loading; ε_{uel} = uniform elongation strain of energy-dissipating bar at f_{uel} under monotonic tension loading. no. 7 = 22M; no. 9 = 29M; no. 11 = 36M; 1 in. = 25.4 mm; 1 ksi = 6.895 MPa.

stress f_{uel} and corresponding uniform elongation strain ε_{uel} and undergone an approximately 0.5% decrease in stress from f_{uel}. The subsequent incremental strains (that is, additional strains after removal of the extensometer) were calculated from the relative displacements of the testing machine crossheads.

The no. 7 (22M) energy-dissipating bars used in specimens 7 through 10 were from a single manufacturing heat (called heat 2 here) but were provided by a different manufacturer than the no. 7 bars in specimens 1 through 6[8] (heat 1). **Figure 4** shows

Energy-dissipating bar	Sample number	Yield strength f_{sy}, ksi	Yield strain ε_{sy},[*] %	Modulus of elasticity E_s, ksi	Ultimate (maximum) strength f_{uel}, ksi	Uniform elongation strain ε_{uel},[†] %	Strain at bar fracture $\varepsilon_{s,fr}$,[‡] %
No. 7 heat 1 (specimens 1 through 6)	1	67.3	0.34	30,689	100.2	12.86	21.28
	2	66.9	0.34	30,680	100.1	14.06	21.36
	3	67.5	0.31	31,135	100.4	13.33	21.21
	Average	67.2	0.33	30,835	100.2	13.42	21.28
No. 7 heat 2 (specimens 7 through 10)	1	68.7	0.44	28,456	99.6	9.59	15.50
	2	69.7	0.47	25,967	99.6	9.19	16.44
	3	69.2	0.47	25,738	99.0	9.02	14.62
	Average	69.2	0.46	26,720	99.4	9.27	15.52
No. 9 (specimen 11)	1	70.1	0.46	27,240	100.2	9.26	12.47
	2	70.2	0.45	27,734	100.5	8.96	12.31
	3	70.1	0.45	28,011	100.3	8.97	12.06
	Average	70.1	0.45	27,662	100.3	9.06	12.28
No. 11 (specimen 12)	1	65.2	0.43	28,120	95.0	10.93	15.75
	2	65.0	0.44	27,440	94.8	11.57	17.76
	3	65.3	0.44	26,811	94.9	10.99	17.61
	Average	65.2	0.44	27,457	94.9	11.16	17.04

Table 3. Energy-dissipating bar properties under monotonic tension

Note: No. 7 = 22M; no. 9 = 29M; no. 11 = 36M; 1 ksi = 6.895 MPa.

[*] O markers in Fig. 4.

[†] Δ markers in Fig. 4.

[‡] ∇ markers in Fig. 4.

the measured monotonic tension stress-strain behaviors for the no. 7, 9, and 11 (22M, 29M, and 36M) energy-dissipating bars and includes the stress-strain behavior of the no. 7 bars for specimens 1 through 6.

The energy-dissipating bar properties are summarized in **Table 3**. The yield strength f_{sy} and strain ε_{sy} for the no. 7 (22M) energy-dissipating bars in specimens 1 through 6 were determined based on the measured stress and strain at the initiation of the yield plateau.[8] The stress-strain behaviors of the no. 7, 9, and 11 (22M, 29M, and 36M) energy-dissipating bars in specimens 7 through 12 did not have a distinct yield plateau. For these bars, the yield strength was determined using the 0.2% offset method in *Standard Test Methods and Definitions for Mechanical Testing of Steel Products* (ASTM A370-17).[12] The modulus of elasticity E_s was calculated as the ratio of the difference between two stresses (50 and 20 ksi [345 and 138 MPa]) within the initial linear-elastic range and the difference between the two corresponding strains. The uniform elongation strain ε_{uel} was determined at the maximum strength f_{uel} of the measured stress-strain behavior. Based on material testing, all of the energy-dissipating bars satisfied all

requirements for ASTM A706 steel, including the minimum elongation requirement (that is, fracture strain $\varepsilon_{s,fr}$) of 12% for Grade 60 (414 MPa) no. 7, 9, and 11 bars.

Figure 4 and Table 3 highlight large variations in the uniform elongation strain ε_{uel} and fracture strain $\varepsilon_{s,fr}$ of the ASTM A706 bars from different heats and for the different bar sizes. Note that the stress-strain curve is typically very flat over the strain range encompassing ε_{uel}, which likely contributes to this variability. Careful consideration should be taken to acquire ASTM A706 reinforcing bars with large fracture strain $\varepsilon_{s,fr}$ for use as energy-dissipating bars crossing gap-opening joints. ACI ITG-5.2[2] specifies a maximum allowable energy-dissipating bar tension strain of $0.85\varepsilon_{uel}$ in the design of gap-opening precast concrete joints. However, because reinforcing bars satisfying ASTM A706 can show great variation in ε_{uel}, validation of energy-dissipating bar connections based on a prescribed absolute value of maximum strain rather than strain as a proportion of ε_{uel} would result in more consistent performance requirements. Accordingly, a target maximum energy-dissipating bar strain of 0.06 in./in. (0.06 mm/mm) was deemed appropriate for the cyclic load validation of the
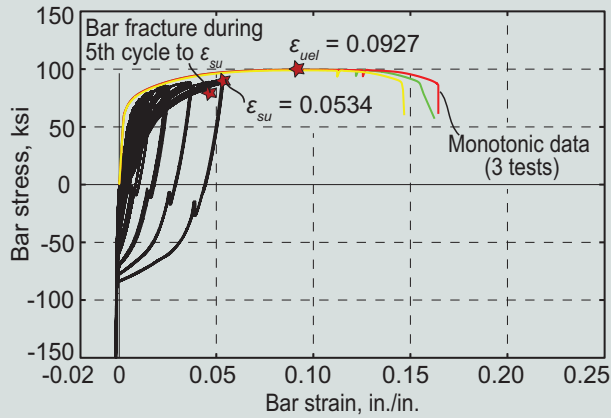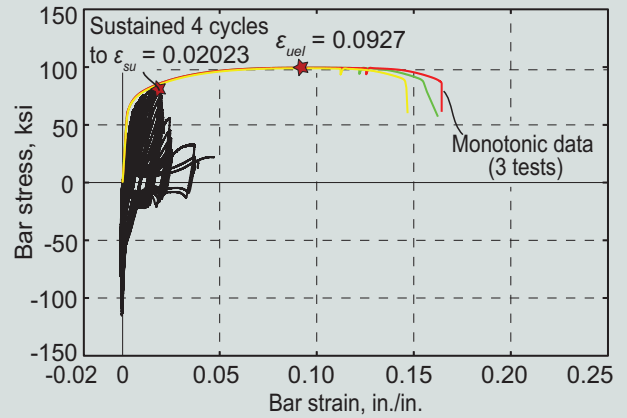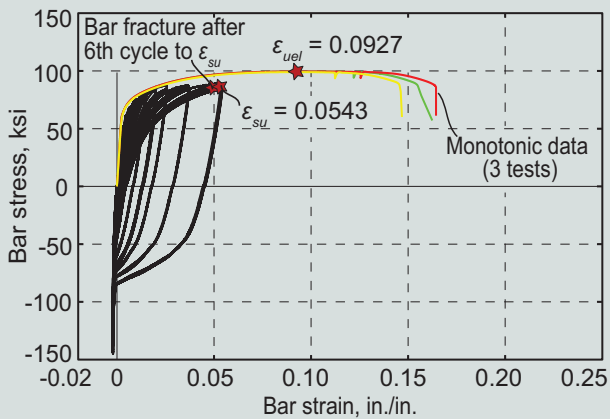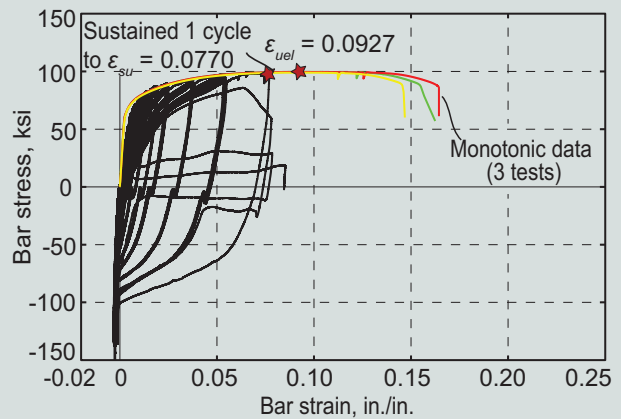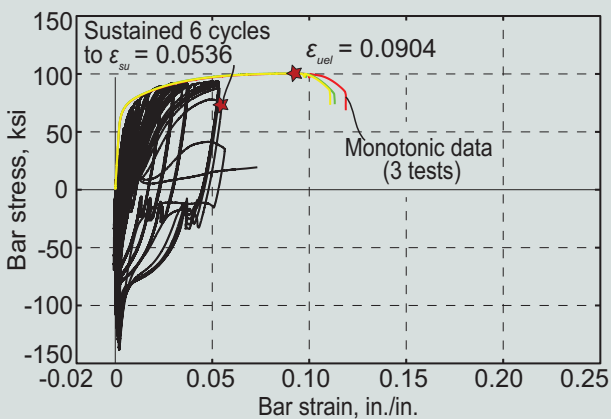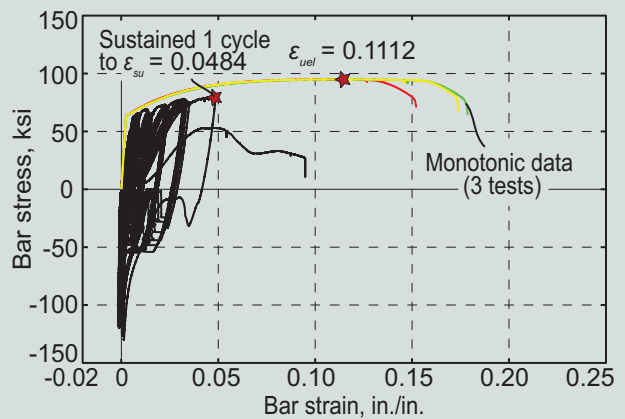
Figure 5. Energy-dissipating bar connection test results showing measured cyclic stress-strain behaviors from specimens 7 through 12. Note: f_{uel} = ultimate (maximum) strength of energy-dissipating bar under monotonic tension loading; ε_{su} = tension strain amplitude (that is, maximum tension strain) of last loading series (that is, last loading increment) before connection failure under cyclic loading; ε_{uel} = uniform elongation strain of energy-dissipating bar at f_{uel} under monotonic tension loading. 1 in. = 25.4 mm; 1 ksi = 6.895 MPa.

Type III connections. This maximum strain value was selected based on the maximum energy-dissipating bar strains from the precast concrete shear wall specimens tested according to ACI ITG-5.1[7] in Smith et al.[4] and the full-scale wall design example in Smith and Kurama.[5]

Energy-dissipating bar connection test results

Figure 5 shows the measured cyclic stress-strain behavior of the energy-dissipating bar from specimens 7 through 12. The corresponding measured monotonic tension stress-strain behaviors from Fig. 4 are superimposed on each cyclic stress-strain plot. As described in Aragon et al.,[8] the bar strains were calculated by dividing the average relative displacement between the wall-panel and foundation blocks with a total estimated unbonded length l_{su}. The average relative displacement was measured as the joint separation from four linear variable displacement transducers (LVDTs). The estimated unbonded length l_{su} of $13d_b$ included $12d_b$ of wrapped length plus an assumed $1d_b$ of additional debonding caused by the cyclic loading of each bar. Even though any debonding likely developed gradually throughout each test, this adjustment was applied to the entire strain history from the LVDTs because the property of greatest interest was the largest tension strain (that is, connection strain capacity) toward the end of the test. The unbonded (wrapped) length of each bar where yielding in tension occurred included two strain gauges (Fig. 1); however, these gauges failed relatively early in each test and thus could not be used to measure the strains throughout the test.

Table 4 provides a summary of the results from the cyclic connection tests, including the total number of sustained loading cycles, accumulated strain, tension strain amplitude (that is, maximum tension strain) of last loading series (that is, last loading increment), number of sustained cycles in the last loading series, and failure mode. Consistent with ACI ITG-5.1,[7] failure was deemed to have occurred during any cycle with a tension stress drop of 20% or greater from the largest tension stress reached in the entire loading history. Thus, the number of sustained cycles in Table 4 indicates the number of cycles where at least 80% of the overall maximum stress was maintained. The accumulated strain represents the total amount of tension and compression strain (in absolute value) that each bar was subjected to during all of the sustained cycles. Any specimen that sustained six cycles at a peak tension strain of 0.06 in./in. (0.06 mm/mm) or greater was deemed to have undergone ductile failure (none of the specimens in Table 4), regardless of the eventual failure mode: either low-cycle fatigue fracture or bond pullout of the energy-dissipating bar.

Failure in specimens 7 and 9 occurred due to low-cycle fatigue fracture of the energy-dissipating bars, which is considered to be a desirable failure mode for the experimental validation of the connection (that is, failure occurs in the bar rather than in the grouted connector). However, the maximum tension strains prior to bar fracture were relatively low (ε_{su} = 0.0534 and 0.0543 in./in. [0.0534 and 0.0543 mm/mm] [$0.58\varepsilon_{uel}$ and $0.59\varepsilon_{uel}$] in specimens 7 and 9, respectively) and did not achieve the target ductility requirement of 0.06 in./in. (0.06 mm/mm). The bar fractures occurred away from the strain gauge locations and thus were not affected by the placement or presence of the gauges. These results show that the maximum allowable strain of $0.85\varepsilon_{uel}$ recommended for the design of energy-dissipating bars in ACI ITG-5.2[2] is not readily achievable by ASTM A706 bars and thus is unconservative for design. Because of the premature energy-dissipating bar fractures, the performance of the different connection grout (GM2) in specimen 7 and the straight connector sleeve in specimen 9 could not be fully tested.

ASTM A706[9] specifications focus on regulating the monotonic stress-strain parameters (minimum elongation, and minimum yield and ultimate tensile strengths) and the chemistry of the bars for weldability. Previous experimental studies[13–15] have shown that there is no correlation between the monotonic stress-strain properties and the low-cycle fatigue performance of ASTM A706 Grade 60 (414 MPa) deformed reinforcing bars. Ghannoum and Slavin[13] therefore suggest

Table 4. Energy-dissipating bar connection test results

Specimen	Total number of sustained cycles	Accumulated strain, in./in.	Strain amplitude of last series ε_{su}	Number of sustained cycles in last series	Failure mode
7	66	1.12	0.0534 ($0.58\varepsilon_{uel}$)	4	Fracture
8	48	0.46	0.0202 ($0.22\varepsilon_{uel}$)	4	Brittle pullout
9	68	1.25	0.0543 ($0.59\varepsilon_{uel}$)	6	Fracture
10	69	1.38	0.0770 ($0.84\varepsilon_{uel}$)	1	Brittle pullout
11	72	1.28	0.0536 ($0.59\varepsilon_{uel}$)	6	Brittle pullout
12	55	0.72	0.0484 ($0.44\varepsilon_{uel}$)	1	Brittle pullout

Note: f_{uel} = ultimate (maximum) strength of energy-dissipating bar under monotonic tension loading; ε_{uel} = uniform elongation strain of energy-dissipating bar at f_{uel} under monotonic tension loading. 1 in. = 25.4 mm.

that additional specifications for the rolling of the bars be introduced in ASTM A706 "to improve the reliability of the low-cycle fatigue performance of reinforcing bars intended for seismic applications." The results from specimens 7 and 9 support this recommendation.

Specimen 8, which used a different connection grout (GM3 with f'_{cg} = 8345 psi [57.5 MPa]), failed through progressive debonding/pullout of the energy-dissipating bar after the first complete cycle to a strain of ε_{su} = 0.0202 in./in. (0.0202 mm/mm) (approximately $0.22\varepsilon_{uel}$). Complete pullout (bond failure and stress drop by more than 20%) occurred after the completion of four cycles at this strain level. Specimens 10 (no. 7 [22M] energy-dissipating bar, f'_{cg} = 7721 psi [53.24 MPa]), 11 (no. 9 [29M] energy-dissipating bar, f'_{cg} = 8595 psi [59.26 MPa]), and 12 (no. 11 [36M] energy-dissipating bar, f'_{cg} = 8310 psi [57.3 MPa]), which used GM2, also failed through bar pullout. In all four specimens, the bond failure developed on a cylindrical surface just outside of the lugs, similar to the bond failure shown in Figure 9 of Aragon et al.[8] for specimen 3. Importantly, the GM3 compressive strength in specimen 8 was similar to many of the GM2 specimens, but bond failure occurred at a very small strain capacity. Conversely, even though GM2 in specimen 10 had the lowest test-day compressive strength of 7721 psi, complete pull-out failure of the energy-dissipating bar occurred after one full cycle at a strain ε_{su} of 0.0770 in./in. (0.0770 mm/mm) ($0.84\varepsilon_{uel}$), thus achieving the target strain of 0.06 in./in. (0.06 mm/mm), though it did not complete the full six cycles necessary to achieve ductile failure. This shows that despite the reduced grout compressive strength, it was possible to develop large tension stresses and strains in the no. 7 energy-dissipating bar over a short bond length of $10d_b$, consistent with the findings in Aragon et al.[8]
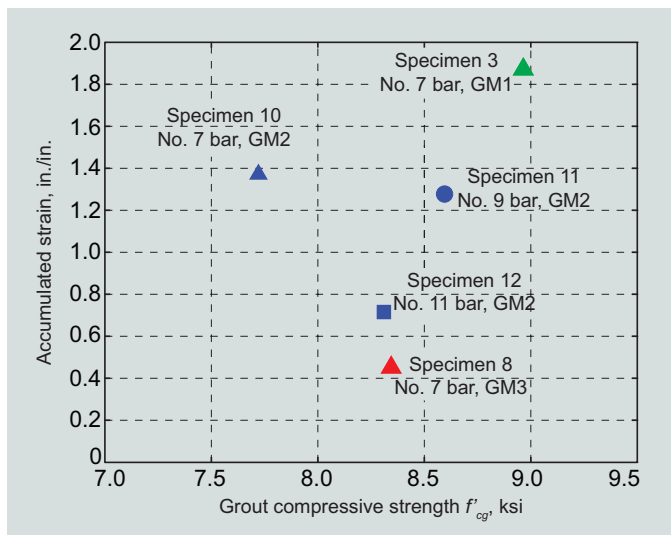
Figure 6 shows the accumulated energy-dissipating bar strain compared with the test-day average compressive strength of the grout f'_{cg} for each specimen that failed by bar pullout (specimens 3,[8] 8, 10, 11, and 12). Comparing specimen 8 (no. 7 [22M] energy-dissipating bar embedded in GM3) with specimen 10 (no. 7 energy-dissipating bar embedded in GM2) shows the inferior performance from GM3 despite its higher compressive strength compared with GM2. This implies that grout properties other than the compressive strength may have contributed to the premature pull-out failure of the energy-dissipating bar in specimen 8, pointing to the need to further study the connection grout as discussed in the following sections. Note that the connection test results were not influenced by the reuse of the foundation block in two tests. This is because any concrete cracking at the top of the foundation block from the first test did not extend to the bottom of the block where the second connector was located. Furthermore, grouting of the second connector was done only after the testing of the first connector was completed and the block was rotated. In the case of specimen 8 with the premature pull-out failure, the foundation block had not been used in a previous test.

Another important observation is that the reduced cyclic strain capacities when comparing specimens 10, 11, and 12 (no. 7, 9, and 11 bars, respectively), all using GM2, indicate that larger-diameter bars resulted in more demanding bond conditions on the connector grout, despite the proportionally increased bond length l_b with the bar diameter d_b (that is, $l_b = 10d_b$). This finding is different from the monotonic pull-out tests described in Steuck et al.,[16] where the effect of bar size on the anchorage of reinforcing bars in grouted straight ducts was found to be small.

Post-test condition of connector grout

To assess the post-test condition of the grout inside each connector sleeve, the two foundation blocks used in specimens 7, 8, 9, and 10 were saw cut along the height of the sleeves in each block (**Fig. 7**). Visual inspections confirmed that the grout was placed uniformly within each connector, with no voids or separation. The cut grout surfaces were subsequently sprayed with alcohol to highlight the crack patterns. All of the cracking was isolated within the connector grout, with no cracks in the surrounding concrete below the top surface of the foundation block. The following observations were made based on the visible crack patterns at different stages during the drying of the alcohol:

- A significant number of cracks developed in the connector grout, but there was no evidence of significant dislocation or slip of the cracked pieces.

- The cracks in the connector grout were generally consistent with the mechanism of bond resistance for cyclic loading described in Eligehausen et al.[17] Inclined cracks developed at the point of contact between the energy-dissipating bar and the grout under loading in tension. The

Figure 6. Accumulated energy-dissipating bar strain plotted against average grout compressive strength for specimens that failed by energy-dissipating bar pullout (bond failure). Note: f'_{cg} = compressive strength of grout at day of energy-dissipating bar connection testing. No. 7 = 22M; no. 9 = 29M; no. 11 = 36M; 1 in. = 25.4 mm; 1 ksi = 6.895 MPa.

Figure 7. Post-test condition of connector grout.

Cracks at middle and bottom of sleeve, with essentially no cracking at top (Specimen 7)

Cracks at middle and bottom of sleeve (Specimen 8)

Cracks at top of sleeve (Specimen 8)

Cracks at top and middle of sleeve, with essentially no cracking at bottom (Specimen 9)

cracks abruptly stopped at the connector sleeve; they did not continue into the foundation block concrete. Upon reversal of loading, the initial cracks closed and inclined cracks nearly perpendicular to the initial cracks developed, resulting in the observed crisscross crack pattern.

- The main distinction in grout crack patterns between the tapered connector with bar fracture (specimen 7) and the tapered connectors with bar pullout (specimens 8 and 10) was that the grout inside the connectors with bar pullout seemed to have more distributed cracking over the sleeve height, whereas the grout inside the connector with bar fracture had almost no cracking near the narrow (top) end of the sleeve. The lack of cracking at the top of the grout cone in specimen 7 is believed to be a result of the confinement provided to the grout due to the tapered shape of the connection. Specimens 8 and 10 also had this confinement effect, but the grout properties in these specimens likely resulted in the additional cracks at the top and the bond failure of the reinforcing bar.

- The grout inside the straight sleeve connector with bar fracture (specimen 9) had cracking near the top and middle of the sleeve height, but no cracks were seen near the bottom. This is consistent with the Eligehausen et al.[17] model, where bond stresses develop closer to the loaded end of the reinforcing bar.

Microscopic characterization of grout

Following the experimental testing of specimens 7 through 12, an additional bag of each grout product (GM1, GM2, and GM3) was mixed per manufacturer instructions to reach a flowable consistency (similar to the grout used in the energy-dissipating bar connectors). Each batch of grout was then cast into $2.0 \times 2.0 \times 2.0$ in. ($50 \times 50 \times 50$ mm) molds and

sent to a materials scientist for microscopic characterization. In general, the results of this characterization did not indicate material differences that were significant enough to cause the performance differences observed in the cyclic energy-dissipating bar connection tests. It was found that GM1 contained quartz-quartzite natural sand with a no. 8 (2.4 mm) mesh maximum size dispersed in portland cement paste with a small amount of fragmental carbonate. The cement was defined as somewhat coarse, and the air content was estimated to be 3% to 4%. The air voids were spherical, small to coarse, and nonuniformly distributed. GM2 was composed of mainly quartz-feldspar natural sand with a no. 30 (0.6 mm) mesh maximum size, distributed in portland cement and fly ash paste. There was a significant amount of fly ash replacement in the grout. The cement was found to be fairly coarse, and the air content was estimated to be 2%. The air voids were spherical, mostly coarse, and very nonuniformly distributed. The composition of GM3 was found to be mainly of quartz-feldspar natural sand with a no. 30 mesh maximum size, dispersed with a small amount of carbonate aggregate in portland cement paste. The cement was somewhat coarse, and the air content was estimated to be 3%. The air voids were spherical, generally small, and slightly nonuniformly distributed.

Monotonic energy-dissipating bar pull-out tests in grout

To further investigate the mechanical properties of each grout (GM1, GM2, and GM3), monotonic bond pull-out tests were conducted. A modified version of ASTM 1081, *Standard Test Method for Evaluating Bond of Seven-Wire Steel Prestressing Strand*,[18] was used. The tests were conducted using ASTM A706 no. 7 (22M) bar samples from the same heat as the energy-dissipating bars in specimens 7 through 10. Each bar was centered in a grouted steel tube with an outside diameter of 5 in. (125 mm) (**Fig. 8**). Three specimens were cast for each
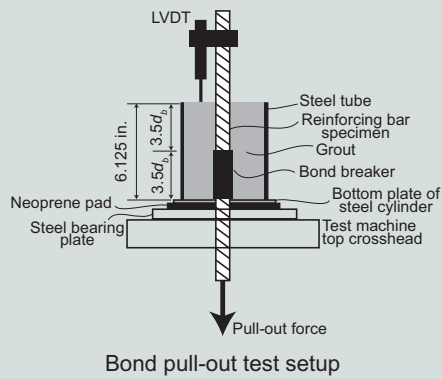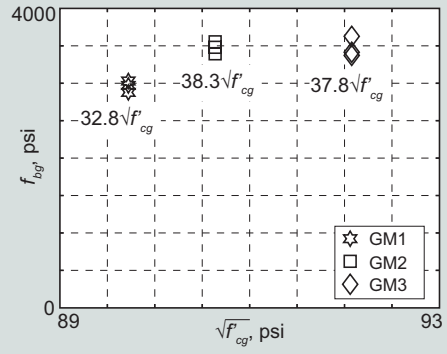
Figure 8. Monotonic bar bond pull-out test and modulus-of-rupture test setup and results for each grout. Note: d_b = nominal diameter of reinforcing bar; f_{bg} = bond strength of grout from monotonic bar pull-out testing; f'_{cg} = compressive strength of grout at day of monotonic bar bond pullout or modulus-of-rupture testing; f_{rg} = modulus-of-rupture strength of grout; LVDT = linear variable displacement transducer. 1 in. = 25.4 mm; 1 psi = 6.895 kPa.

grout product, using a single bag of prepackaged grout mixed per manufacturer instructions to reach a flowable consistency. The bond strength tests for each grout were accompanied by three $2.0 \times 2.0 \times 2.0$ in. ($50 \times 50 \times 50$ mm) grout cube compressive strength tests.

The no. 7 (22M) bar in each monotonic pull-out test extended out from both ends of the grout-filled steel tube. The thickness of the tube wall was 0.119 in. (3.02 mm) in accordance with ASTM 1081. The tube may have provided confinement and affected the bond strength; however, as each grout was cast and tested under the same conditions (for example, same tube thickness), the confinement was the same for all of the pull-out tests. The tube with the embedded bar was placed over a neoprene pad and a thick steel bearing plate above the top crosshead of a hydraulic universal testing machine. An LVDT was attached to the top free end of the bar to record the slip relative to the top surface of the grout. The bottom end of the bar was anchored to the bottom crosshead of the testing machine using wedge grips. A tension force was applied on the bar by moving the top crosshead of the testing machine upward at a constant rate of 0.1 in./min (2.5 mm/min). The tests were conducted at a grout age of 14 days, after the grout samples had reached average compressive strengths f'_{cg} over 8000 psi (55 MPa).

The bond strength f_{bg} was calculated as the average stress between the bar and the surrounding grout along the embedded length of the bar.

$$f_{bg} = \frac{P_f}{\pi d_b l_b}$$

where

P_f = maximum pull-out force

d_b = nominal diameter of bar

l_b = bond length of bar

A short bond length l_b of $3.5d_b$ (3.0625 in. [77.79 mm]) was chosen to prevent yielding of the bar prior to slip to remove this variable from the monotonic bond strength tests. Beyond this bond length, each bar was unbonded from the grout (by wrapping the bar inside a plastic sleeve) over a length of $3.5d_b$, resulting in a total height of $7.0d_b = 6.125$ in. (155.6 mm) for the steel tube. GM1 (Fig. 8) and GM3 experienced slight upward expansion at the top of the tube (where the grout was open to air) during curing (approximately 0.25 and 0.10 in. [6.4 and 2.5 mm], respectively), which was included in the total bond length.

Figure 8 shows the data from the pull-out tests, where each point represents the bond strength f_{bg} from a single pull-out specimen plotted against the average $\sqrt{f'_{cg}}$ from the three companion grout cube compressive strength specimens. **Table 5** gives the average bond strength f_{bg} along with the average

Table 5. Monotonic bond pull-out tests and modulus-of-rupture tests of grout

Grout	Bond pull-out tests						Modulus-of-rupture tests					
	Bond strength f_{bg}, psi				Average square root of grout compressive strength $\sqrt{f'_{cg}}$, psi	$\dfrac{f_{bg}}{\sqrt{f'_{cg}}}$, with numerator and denominator in psi	Modulus-of-rupture strength f_{rg}, psi				Average square root of grout compressive strength $\sqrt{f'_{cg}}$, psi	$\dfrac{f_{rg}}{\sqrt{f'_{cg}}}$, with numerator and denominator in psi
	Specimen			Average			Specimen			Average		
	1	2	3				1	2	3			
GM1	2880	3000	2940	2940	89.7	32.8	760.3	754.2	775.2	763.3	90.0	8.5
GM2	3480	3415	3515	3470	90.6	38.3	563.0	667.6	755.8	662.1	95.8	6.9
GM3	3620	3425	3410	3485	92.1	37.8	672.4	629.4	534.5	612.1	90.4	6.8

Note: 1 psi = 6.895 kPa.

$\sqrt{f'_{cg}}$ for the three grout products. Despite the increasing grout compressive strength, the bond strength did not increase from GM2 to GM3. However, overall, the differences in the monotonic bond strength f_{bg} were not representative of the extremely poor performance of GM3 during the cyclic Type III connection tests (Fig. 6). These results attest to the importance of conducting cyclic tests when evaluating grouted energy-dissipating bar connectors for seismic applications.

Modulus-of-rupture tests of grout

A significant amount of cracking occurred in the energy-dissipating bar connector grout (Fig. 7), which likely affected its performance. As a measure of tensile strength, the 28-day modulus-of-rupture (MOR) strength f_{rg} of each grout product was determined by testing three grout beams under three-point bending (Fig. 8). The three MOR beams (and accompanying $2.0 \times 2.0 \times 2.0$ in. [$50 \times 50 \times 50$ mm] cubes for compressive strength testing) for each grout product were cast using a single bag of prepackaged grout that was mixed per manufacturer instructions to reach a flowable consistency. The MOR beams measured $3.67 \times 3.67 \times 14.0$ in. ($93.2 \times 93.2 \times 360$ mm), with a span length L of 11 in. (280 mm), satisfying *Standard Test Method for Flexural Strength of Concrete (Using Simple Beam with Center-Point Loading)* (ASTM C293)[19] requirements.

Each MOR beam was placed on its side with respect to its casting configuration so that the support and loading reaction rods could rest against smooth formwork-finished surfaces as specified by ASTM C293. The beam was loaded at a rate of 433 lb/min (197 kg/min) (corresponding to a stress increase of 150 psi/min [1030 kPa/min] on the extreme tension face) using a hydraulic universal testing machine.

The MOR strength f_{rg} was calculated as the following:

$$f_{rg} = \frac{3PL}{2bh^2}$$

where

P = maximum applied load at failure

L = span length of MOR beam (11.0 in. [280 mm])

b = width of MOR beam at ruptured section

h = depth of MOR beam at ruptured section

Figure 8 and Table 5 show the 28-day f_{rg} values from each set of three tests along with the average $\sqrt{f'_{cg}}$ values from the accompanying 2.0×2.0 in. $\times 2.0$ in. ($50 \times 50 \times 50$ mm) grout cubes. The MOR strength of 8.5 $\sqrt{f'_{cg}}$ for GM1 was significantly greater than the MOR strengths of 6.9 $\sqrt{f'_{cg}}$ and 6.8 $\sqrt{f'_{cg}}$ for GM2 and GM3, respectively. The largest variability between the three MOR specimens occurred for GM2, while the smallest variability occurred for GM1.Similar to the monotonic pull-out tests, these MOR test results did not explain the significantly inferior performance of GM3 compared with GM2 in the cyclic Type III connection tests. Because an important goal of this nonproprietary connection is for it to be used without requiring a specific grout product, more research needs to be conducted before it can be used in practice. Given the wide performance differences observed from the cyclic connection tests and the lack of a reliable method to identify these differences from simple grout tests (for example, compression/tension tests or monotonic pull-out tests), it may be necessary to increase the bond length of the Type III connection to achieve this objective. Given the similar compressive and tensile strengths of the three grout products, achieving a certain grout strength does not necessarily indicate satisfactory bond performance with the reinforcing bar under cyclic loading.

Strains in foundation tie reinforcement

The 28-day compressive strength of the foundation block
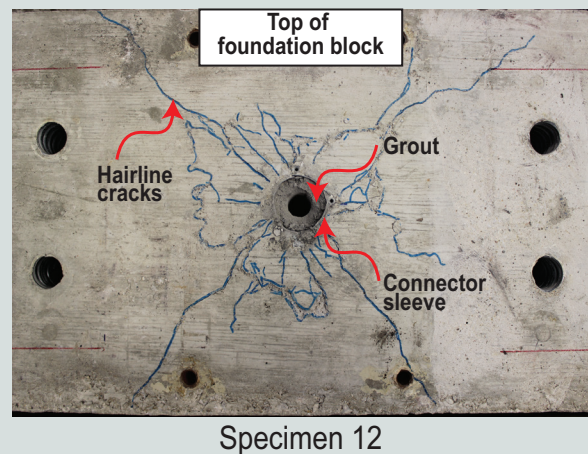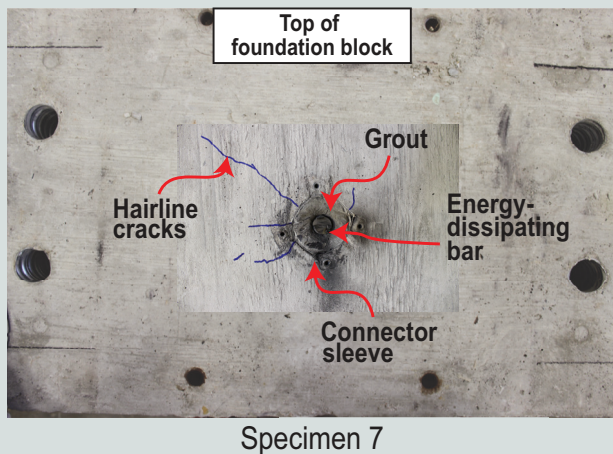
Figure 9. Cracking at top of foundation block.

concrete for specimens 7 through 12 $f'_{c,28d}$ was 4851 psi (33.45 MPa). A few short hairline cracks were observed extending outward from the edge of the connector sleeve at the top of the foundation block after the connection testing in specimens 7 through 10 with no. 7 (22M) energy-dissipating bars (**Fig. 9**). The largest measured foundation block steel strains in these specimens were 0.00203 and 0.00163 in./in. (0.00203 and 0.00163 mm/mm) in the vertical and horizontal tie reinforcement, respectively, which were close to the yield strain of the bars (ε_{sy} = 0.00224 in./in. [0.00224 mm/mm]).

The cracking in the foundation block of specimens 11 and 12 (with the larger energy-dissipating bar sizes) was more extensive (both in length and number of cracks); however, the cracks remained hairline width (Fig. 9). The largest measured steel strains in specimen 11, which used a no. 9 (29M) energy-dissipating bar, were 0.00232 and 0.00114 in./in. (0.00232 and 0.00114 mm/mm) in the vertical and horizontal tie reinforcement, respectively. For specimen 12 (with no. 11 [36M] energy-dissipating bar), the largest measured steel strains were 0.00231 and 0.00178 in./in. (0.00231 and 0.00178 mm/mm) in the vertical and horizontal tie reinforcement, respectively. As discussed in Aragon et al.,[8] the tie reinforcement was not designed with any overstrength (that is, the provided tie reinforcement areas were very close to the required areas from the strut-and-tie model); therefore, a small amount of yielding was deemed possible. The hairline width of the cracks and the steel strains close to the yield strain of the bars (ε_{sy} = 0.00224 in./in. [0.00224 mm/mm]) validated the strut-and-tie design of the foundation reinforcement. In a real-world application, a capacity reduction factor should be used to incorporate an appropriate factor of safety to the tie reinforcement design.

Conclusion

This paper extends previous experimental results[8] of a Type III cementitious-grouted connection for energy-dissipating deformed steel reinforcing bars at gap-opening joints in precast concrete structures subjected to seismic loads. Six

connection tests and accompanying energy-dissipating bar and connector grout material tests were conducted to investigate the effect of the following parameters on the connection: grout product, grout strength, energy-dissipating bar diameter, and energy-dissipating bar heat. The conclusions from these test results are listed. Note that these conclusions may be limited to the specimens and materials tested, as well as the applied loading conditions (that is, uniaxial loading) on the connections. Also, as reflected by the title, the primary focus of this paper is on the effects of grout and energy-dissipating bar properties. As such, the findings related to these effects are important and have implications beyond the Type III connectors investigated.

- Large variations were measured in the monotonic uniform elongation strain ε_{uel} and fracture strain $\varepsilon_{s,fr}$ of ASTM A706 bars from different heats and of different sizes. ACI ITG-5.2 specifies a maximum allowable energy-dissipating bar tension strain (for the design of gap-opening precast concrete joints) as a proportion of ε_{uel} (specifically, $0.85\varepsilon_{uel}$). Because bars satisfying ASTM A706 can show great variation in ε_{uel}, a prescribed value of the maximum allowable energy-dissipating bar tension strain (not as a proportion of ε_{uel}) would result in more consistent performance.

- In general, careful consideration should be taken to acquire ASTM A706 reinforcing bars with large fracture strain $\varepsilon_{s,fr}$ for use as energy-dissipating bars across gap-opening joints.

- The maximum strain capacity of two connection specimens (specimens 7 and 9) was limited by the low-cycle fatigue fracture of the energy-dissipating bar, which is considered to be a desirable failure mode for the experimental validation of the connection (that is, failure occurs in the bar rather than in the grouted connector). However, the maximum tension strains prior to bar fracture were relatively low (approximately $0.6\varepsilon_{uel}$), demonstrating that the maximum allowable strain of $0.85\varepsilon_{uel}$ recommended

for the design of energy-dissipating bars in ACI ITG-5.2 is unconservative. These results support previous research recommendations from Ghannoum and Slavin[13] that additional requirements be introduced in ASTM A706 to improve the low-cycle fatigue performance of reinforcing bars intended for seismic applications.

- The maximum strain capacity of the other four specimens (specimens 8, 10, 11, and 12) was limited by bond failure (that is, energy-dissipating bar pullout) inside the grouted connector sleeve, demonstrating that the grout properties are very important in determining the failure mode of the connection and resulting strain capacity. The compressive strength of the grout in specimen 8 (GM3) was similar to the compressive strength of GM2 used in the other specimens, but GM3 resulted in bond failure at a very small strain capacity. Conversely, even though GM2 in specimen 10 had the lowest compressive strength, pull-out failure occurred at a strain of ε_{su} = 0.0770 in./in. (0.0770 mm/mm), thus reaching the target strain of 0.06 in./in. (0.06 mm/mm), though not completing the full six cycles. This shows that despite the reduced grout strength, it was possible to develop large tension stresses and strains in the energy-dissipating bar over a short bond length of $10d_b$ (consistent with the findings in Aragon et al.[8]), and that grout properties other than the compressive strength may be important in determining the connection performance.

- The reduced cyclic strain capacities when comparing specimens 10, 11, and 12 (no. 7, 9, and 11 [22M, 29M, and 36M] bars, respectively, all using GM2) indicate that larger-diameter bars resulted in more-demanding conditions on the connector grout, despite the proportionally increased bond length l_b with the bar diameter d_b (that is, $l_b = 10d_b$).

- The specimens that were saw cut along the height of the connector sleeve after the connection testing showed significant cracking of the connection grout; however, there was no evidence of dislocation or slip of the cracked grout pieces. The tapered connection with energy-dissipating bar fracture (specimen 7) had almost no cracking near the narrow (top) end of the sleeve, whereas the connections with bar pullout (specimens 8 and 10) had more distributed cracking over the entire sleeve height.

- Monotonic energy-dissipating bar bond pull-out tests and grout modulus-of-rupture tests showed relatively small differences between the three different grout products. These tests were not conclusive in identifying the reasons for the significantly inferior performance of GM3 during the cyclic connection tests. The results of a microscopic characterization also did not indicate material differences between the three grout products that were significant enough to cause the performance differences observed in the cyclic energy-dissipating bar connection tests.

- The differences between the bond performance of the three grout products when tested under monotonic loading compared with the bond performance under cyclic loading attest to the importance of conducting cyclic tests to evaluate grouted energy-dissipating bar connectors for seismic application. Further, given the similar compressive and tensile strengths of the three grout products, it can be concluded that achieving a certain grout strength does not necessarily ensure satisfactory bond performance with reinforcing bar.

- Given the wide performance differences observed from the cyclic connection tests with different grout products and the lack of a reliable method to identify these differences from simpler tests (for example, grout compression tests or monotonic pull-out tests), it may be necessary to increase the bond length of this nonproprietary Type III connection.

- Future tests using a wider range of parameters (for example, increased energy-dissipating bar bond length) as well as more realistic multidirectional loading conditions (that is, combined axial and lateral loads at a gap-opening joint with rotation) are needed. Other parameters that need to be tested include additional variations of the connector sleeve taper angle, connector edge distance, construction tolerances, inaccuracies, and errors, as well as energy-dissipating bar groups tested in representative structural wall, column, or pier details and configurations.

- Concrete cracking around (outside) the connector sleeve at the top of the foundation remained hairline width, and the maximum tension strains in the foundation tie reinforcement were close to the yield strain of the bars. These results validated the strut-and-tie design of the connection tie reinforcement in the foundation.

Acknowledgments

Erico Inc. Any opinions, findings, and conclusions or recommendations expressed in the paper are those of the authors and do not necessarily reflect the views of the individuals and organizations acknowledged here.

References

1. Joint ACI-ASCE Committee 550. 2014. *Design Specification for Unbonded Post-tensioned Precast Concrete Special Moment Frames Satisfying ACI 374.1.* ACI 550.3-13. Farmington Hills, MI: ACI.

2. ACI (American Concrete Institute) Innovation Task Group 5. 2009. *Requirements for Design of a Special Unbonded Post-tensioned Precast Shear Wall Satisfying ACI ITG-5.1 and Commentary.* ACI ITG-5.2. Farmington Hills, MI: ACI.

3. Marsh, M. L., J. F. Stanton, M. Wernli, M. O. Eberhard, B. E. Garrett, and M. D. Weinert. 2011. "Application of Accelerated Bridge Construction Connections in Moderate-to-High Seismic Regions." NCHRP (National Cooperative Highway Research Program) report 698. Washington, DC: Transportation Research Board. https://doi.org/10.17226/14571.

4. Smith, B. J., Y. C. Kurama, and M. J. McGinnis. 2012. "Hybrid Precast Wall Systems for Seismic Regions." Structural engineering research report NDSE-2012-01. Department of Civil and Environmental Engineering and Earth Sciences, University of Notre Dame, Notre Dame, IN. https://www3.nd.edu/~ykurama/REPORT_NDSE-12-01.pdf.

5. Smith, B. J., and Y. C. Kurama. 2014. "Seismic Design Guidelines for Solid and Perforated Hybrid Precast Concrete Shear Walls." *PCI Journal* 59 (3): 43–49.

6. ACI Committee 318. 2014. *Building Code Requirements for Structural Concrete (ACI 318-14) and Commentary (ACI 318R-14).* Farmington Hills, MI: ACI.

7. ACI Innovation Task Group 5. 2007. *Acceptance Criteria for Special Unbonded Post-tensioned Precast Structural Walls Based on Validation Testing and Commentary.* ACI ITG-5.1. Farmington Hills, MI: ACI.

8. Aragon, T. A., Y. C. Kurama, and D. F. Meinheit. 2017. "A Type III Grouted Seismic Connector for Precast Concrete Structures." *PCI Journal* 62 (5): 75–88.

9. ASTM Subcommittee A01.05. 2016. *Standard Specification for Deformed and Plain Low-Alloy Steel Bars for Concrete Reinforcement.* ASTM A706/A706M. West Conshohocken, PA: ASTM International.

10. ASTM Subcommittee A01.05. 2016. *Standard Specification for Deformed and Plain Carbon-Steel Bars for Concrete Reinforcement.* ASTM A615/A615M. West Conshohocken, PA: ASTM International.

11. ASTM Subcommittee C09.43. 2014. *Standard Specification for Packaged Dry, Hydraulic-Cement Grout (Nonshrink).* ASTM C1107/C1107M. West Conshohocken, PA: ASTM International.

12. ASTM Subcommittee A01.13. 2017. *Standard Test Methods and Definitions for Mechanical Testing of Steel Products.* ASTM A370. West Conshohocken, PA: ASTM International.

13. Ghannoum, W. M., and C. M. Slavin. 2016. "Low-Cycle Fatigue Performance of High-Strength Steel Reinforcing Bars." *ACI Materials Journal* 113 (6): 803–814.

14. Hawileh, R., A. Rahman, and H. Tabatabai. 2010. "Evaluation of the Low-Cycle Fatigue Life in ASTM A706 and A615 Grade 60 Steel Reinforcing Bars." *Journal of Materials in Civil Engineering* 22 (1): 65–76.

15. Brown, J., and S. K. Kunnath. 2004. "Low-Cycle Fatigue Failure of Reinforcing Steel Bars." *ACI Materials Journal* 101 (6): 457–466.

16. Steuck, K. P., M. O. Eberhard, and J. F. Stanton. 2009. "Anchorage of Large-Diameter Reinforcing Bars in Ducts." *ACI Structural Journal* 106 (4): 506–513.

17. Eligehausen, R., E. P. Popov, and V. V. Bertero. 1983. "Local Bond Stress-Slip Relationships of Deformed Bars under Generalized Excitations." Report UCB/EERC-83/23. University of California, Berkeley, CA.

18. ASTM Subcommittee A01.05. 2015. *Standard Test Method for Evaluating Bond of Seven-Wire Steel Prestressing Strand.* ASTM A1081/A1081M. West Conshohocken, PA: ASTM International.

19. ASTM Subcommittee A09.61. 2016. *Standard Test Method for Flexural Strength of Concrete (Using Simple Beam with Center-Point Loading.* ASTM C293/C293M. West Conshohocken, PA: ASTM International.

Notation

b = width of grout modulus-of-rupture beam at ruptured section

d_b = nominal diameter of reinforcing bar

E_s = modulus of elasticity of reinforcing bar

f_{bg} = bond strength of grout from monotonic bar pull-out testing

f'_{cg} = compressive strength of grout at day of energy-dis-

sipating bar connection testing, monotonic bar bond pull-out testing, or grout modulus-of-rupture testing

$f'_{c,28d}$ = compressive strength of foundation and wall-panel block concrete at 28 days

$f'_{cg,28d}$ = compressive strength of grout at 28 days

f_{rg} = modulus-of-rupture strength of grout

$f_{s,fr}$ = stress of energy-dissipating bar at fracture under monotonic tension loading

f_{sy} = yield strength of energy-dissipating bar under monotonic tension loading

f_{uel} = ultimate (maximum) strength of energy-dissipating bar under monotonic tension loading

h = depth of grout modulus-of-rupture beam at ruptured section

h_f = height of foundation block

h_w = height of wall-panel block

L = span length of grout modulus-of-rupture beam

l_b = embedment (bond) length of energy-dissipating bar

l_f = length of foundation block

l_{su} = total unbonded length of energy-dissipating bar (that is, wrapped length plus additional debonded length expected under cyclic loading)

l_{sw} = wrapped length of energy-dissipating bar

l_w = length of wall-panel block

P = maximum applied load at failure of grout modulus-of-rupture beam

P_f = maximum pull-out force for monotonic pull-out bar specimen

t_w = thickness of wall-panel block

w_f = width of foundation block

$\varepsilon_{s,fr}$ = strain of energy-dissipating bar at fracture under monotonic tension loading

ε_{su} = tension strain amplitude (that is, maximum tension strain) of last loading series (that is, last loading increment) before connection failure under cyclic loading

ε_{sy} = yield strain of energy-dissipating bar and tie reinforcement under monotonic tension loading

ε_{uel} = uniform elongation strain of energy-dissipating bar at f_{uel} under monotonic tension loading

θ_d = taper angle of energy-dissipating bar connector sleeve

About the authors

Theresa Aragon, PhD, is a faculty member in the School of Math, Science and Engineering at Central New Mexico Community College in Albuquerque, N.Mex.

Yahya Kurama, PhD, PE, is a professor in the Department of Civil and Environmental Engineering and Earth Sciences at the University of Notre Dame in Notre Dame, Ind.

Donald Meinheit, PhD, PE, SE, is a principal at Wiss, Janney, Elstner Associates Inc. in Chicago, Ill.

Abstract

This paper investigates the effects of grout properties and energy-dissipating steel reinforcing bar properties on the performance of a grouted Type III connection for gap-opening joints of precast concrete structures subjected to seismic displacements. This Type III connection offers the potential for a high-performance yet simple nonproprietary, low-cost system that allows Grade 60 (414 MPa) energy-dissipating ductile deformed reinforcing bars to reach close to their ultimate tensile strength and strain capacity under cyclic loading in a short grouted embedment length. The use of short grouted connections simplifies the construction of precast concrete structures because protruding bar lengths from precast concrete members can be minimized, and field-grouting lengths can be reduced. The test parameters investigated were the grout product, grout strength, energy-dissipating bar size, and energy-dissipating bar heat. It was found that the grout used in the connector sleeve and low-cycle fatigue fracture of the energy-dissipating bar can limit the deformation capacity of the connection. Additional requirements should be introduced in ASTM A706 to improve the low-cycle fatigue performance of reinforcing bars intended for seismic applications. Furthermore, it may be necessary to increase the bond length of the energy-dissipating bar for this nonproprietary connection to be used without the requirement for a specific grout product.

Keywords

ASTM A706, deformed reinforcing bar, energy-dissipating steel bar, gap-opening joint, grouted seismic connector, low-cycle fatigue fracture, Type III connection, uniform elongation strain.

Review policy

This paper was reviewed in accordance with the Precast/Prestressed Concrete Institute's peer-review process.

Reader comments

Please address any reader comments to *PCI Journal* editor-in-chief Emily Lorenz at elorenz@pci.org or Precast/Prestressed Concrete Institute, c/o *PCI Journal*, 200 W. Adams St., Suite 2100, Chicago, IL 60606.